

Synthesis of Horseradish Peroxidase-Gold Nanoparticle Conjugate through Green Route

LOVNISH SIYAL¹, BENU KUMAR¹, RANJIT KUMAR² and RACHANA SAHNEY^{1,*}

¹Amity Institute of Biotechnology, Amity University Uttar Pradesh, Noida-201313, India

²Amity Institute of Nanotechnology, Amity University Uttar Pradesh, Noida-201313, India

*Corresponding author: Fax: +91 120 2431878; Tel.: +91 120 2432780 thru 85; E-mail: rachanasahney@gmail.com; rsahney@amity.edu

Received: 26 December 2019;

Accepted: 15 February 2020;

Published online: 29 April 2020;

AJC-19863

Synthesis of horseradish peroxidase-gold nanoparticle conjugates (HRP-AuNPs) has been studied for the development of biofunctionalized gold nanoparticles (AuNPs) through biogenic route. Herein, horseradish peroxidase enzyme has been used to synthesize gold nanoparticles at room temperature in tricine buffer. The morphology and size distribution of HRP-AuNPs conjugates were obtained by different techniques including dynamic light scattering (DLS), UV-visible (UV-vis) spectrophotometry, scanning electron microscopy (SEM) and energy dispersive X-ray analysis (EDX). The enzyme activity of HRP-AuNP conjugate was compared with free enzyme to determine their catalytic efficiency. The results suggest that HRP-AuNP conjugates are monodisperse particles with average hydrodynamic diameter of 83.93 ± 2.1 nm, zeta potential of about -18.4 ± 1.1 mV and higher enzyme activity towards H_2O_2 as compared to free horseradish peroxidase. These biofunctionalized gold nanoparticles could act as tag or labeling agent for various applications.

Keywords: Horseradish peroxidase, Gold nanoparticle, Zeta potential, Michaelis-Menten constant.

INTRODUCTION

Bio-functionalized gold nanoparticles (AuNPs) are important for development of different nanomaterials and biological systems and their applications in various fields [1-3]. Biofunctionalized AuNPs are widely used in photothermal therapy [4], biological imaging [5] and in cancer diagnostics [6]. On the other hand, a strong localized surface plasmon resonance (LSPRs) [7], which appears in AuNPs at ultraviolet, visible and near infrared wavelengths, promotes their applications in surface enhanced Raman spectroscopy (SERS), metal enhanced fluorescence (MEF) [8] and in the construction of photodiodes, solar cells and light emitting diodes (LEDs) [9]. Biofunctionalization simply involves bonding of biomolecules to AuNPs by chemical or biological means which further enhances stability and application of AuNPs. Various methods have been developed for the synthesis of AuNPs. These methods can be classified into three categories *i.e.* (a) chemical, (b) physical and (c) biological method of synthesis [10,11]. In chemical method, a commonly used method is Turkevich method [12], where gold precursor are reduced in an aqueous environment by application of chemical reducing agents and then functionalized by different

ligands using intricate chemistries. Similarly, different physical method of AuNP synthesis involves the use of radiation for the reduction of gold salts (*i.e.* $HAuCl_4$), for example, laser ablation, ultraviolet (UV) irradiation, γ -irradiation, microwave assisted, ultrasonic irradiation and photochemical methods [13-16]. But physical method also requires high-end and costly instrumentation in the first step of AuNPs synthesis. On the other hand, biological method of synthesis is based on the reduction of gold salts (*i.e.* $HAuCl_4$) by biomolecules, which is environmental friendly and cost-effective as compared to other two methods of synthesis [11,17]. Biomolecules that have been used for the growth of AuNPs include plant/plant extract and microbes like viruses, fungi, *etc.* [18-21]. Variety of purified biomolecules including proteins, peptides, amino acids, saccharides and nucleic acids have been engaged for the production and functionalization of nanosized materials [22-30]. Commercially available enzymes have been utilized for the synthesis of AuNPs due to their ease of availability and diverse functionality. Enzymes that have been used for the reduction of AuNPs are laccase [31], trypsin [32], β -glucosidase [33], pepsin [34] and serrapeptase [35]. Enzymes used in the fabrication of AuNPs acts as reducing agent as well as stabilizing agent and get

adsorbed onto nanoparticle surface [36-42]. Due to adsorption of enzyme on gold nanoparticle surface their spatial conformation might be affected leading to alteration in catalytic activity of enzyme. The changed catalytic activity of enzymes can be taken as an advantage to develop various optical and electrochemical sensing devices [43-47]. Hence, a development of reliable experimental protocol for the synthesis of nanoparticles over a range of chemical compositions, sizes and high monodispersity is one of the challenging issues in current nanotechnology.

This study reports a simple, facile green method for horseradish peroxidase (HRP) mediated AuNPs synthesis in buffer system at room temperature, which results into HRP capped gold nanoparticles (HRP-AuNPs) showing better enzyme catalysis towards hydrogen peroxide. The morphology and size distribution of HRP-AuNPs were obtained by different experimental studies including dynamic light scattering (DLS), UV-visible, scanning electron microscopy (SEM) and energy dispersive X-ray analysis (EDX). The enzyme activity of HRP was studied to determine the catalytic efficiency of HRP-AuNPs.

EXPERIMENTAL

Horseradish peroxidase (HRP; EC 1.11.1.7, 180 U/mg) enzyme was purchased from Sisco Research Laboratories Pvt. Ltd. (SRL), India. Hydrogen peroxide (H₂O₂) and HCl were procured from Fisher Scientific, USA. Tricine buffer was obtained from GCC Biotech (I) Pvt. Ltd., India. Hydrogen tetrachloroaurate(III) (HAuCl₄·3H₂O) was purchased from CDH (P) Ltd., India. All chemicals were used as received without any further purification. Milli-Q water was used in all the experiments obtained from Merck Millipore.

Synthesis of HRP stabilized AuNPs: All the glasswares were initially cleaned with aqua regia and washed repeatedly with Milli-Q water before use. In a 15 mL glass vial containing small magnetic bead, deionized water (5 mL) was taken. Horseradish peroxidase dissolved in tricine buffer (1 mg/mL; pH 9) was added. Simultaneously, HAuCl₄·3H₂O (0.96 mM) was added and then the reaction mixture was stirred at room temperature until colour changes in 14 h (approximately).

UV-visible characterization of HRP-AuNPs: An aliquot of ruby red sample (2 mL) synthesized in present study was placed in a quartz cuvette and UV-visible spectrum of HRP-AuNPs was recorded using an Ocean Optics spectrophotometer (DH-mini) between 300 to 800 nm. Spectrum of developed HRP-AuNPs was measured at a resolution of 1 cm.

Dynamic light scattering (DLS) and zeta potential measurement: A ruby red sample (2 mL) containing HRP-AuNPs was placed in the quartz cuvette and analyzed using Malvern Zeta-sizer-Nano S90 (Malvern, UK) instrument with detector receiving scattered light at 90°, controlled by Dispersion Technology Software (DTS 5.03, Malvern, UK) to estimate the mean hydrodynamic diameter and the polydispersity index (PDI). Mean hydrodynamic diameter and intensity averaged size distributions were obtained from the raw data using the general-purpose inverse Laplace transform method provided in the instrument software. The PDIs were estimated from cumulant analysis provided with the instrument software.

SEM and EDX analysis of HRP-AuNPs: Particle morphology and elemental analysis of HRP-AuNPs were conducted by using scanning electron microscope (Model: ZEISS EVO 18) equipped with energy dispersive X-ray (EDX) spectrometer. Sample was drop coated onto the glass surface and then dried using nitrogen gas under room temperature for analysis.

FTIR analysis: Functional groups present in the HRP enzyme and HRP-AuNPs bioconjugate were analyzed through FTIR spectroscopy (Bruker Tensor 37). A drop of sample was mounted in the center of the stage for analysis. FTIR spectra are analyzed in the range of 4000-500 cm⁻¹.

Enzyme assay of HRP capped AuNP: Enzyme catalysis of hydrogen peroxide with free HRP enzyme and HRP-AuNPs conjugate were studied by measuring the changes in absorbance at 460 nm due to *o*-dianisidine oxidation in the presence of H₂O₂ and enzyme [48]. In a typical experiment, tricine buffer at pH 6 (0.1M) containing 1% *o*-dianisidine (2.5 mL) and H₂O₂ (0.1 mL) with appropriate concentration were taken in a tube. The reaction was initiated by adding 0.1 mL of horseradish peroxidase enzyme solution at room temperature and absorbance was measured at 460 nm. The enzyme loading efficiency and loading capacity of the gold nanoparticles were calculated as follows:

$$\text{Enzyme loading efficiency} = \frac{W_A}{W_T} \times 100 \quad (1)$$

where W_A = weight of HRP capped on AuNPs (g); W_T = weight of total HRP (g).

$$\text{Loading capacity} = \frac{W_A}{W_{Au}} \quad (2)$$

where W_A = weight of HRP capped on AuNPs (g); W_{Au} = weight of gold nanoparticles (g).

The per cent immobilization for HRP-AuNPs conjugates was calculated using the following equation:

$$\text{Immobilization (\%)} = \frac{\text{Specific activity of HRP capped on AuNP}}{\text{Specific activity of free HRP}} \times 100$$

RESULTS AND DISCUSSION

UV-visible analysis of synthesized HRP-AuNP: Gold nanoparticles (AuNPs) have localized electrons in their conduction band which resonate upon interacting with light. This phenomenon is known as the localized surface plasmon resonance (LSPR) due to which AuNPs showed an absorption maxima between 500-600 nm [7]. Fig. 1 shows the spectrum of HRP-AuNP conjugates with maximum absorption at 556 nm wavelength due to LSPR. Thus, it confirms the formation of HRP-AuNP.

Dynamic light scattering (DLS) and zeta potential of HRP-AuNP: A DLS characterization is used to determine the average size and distribution of particles in aqueous solution [49]. The average size of HRP-AuNP synthesized was found to be 83.93 ± 2.1 nm (Fig. 2). The zeta potential of synthesized HRP-AuNP conjugates is essential to determine because zeta potential is a very reliable parameter for the measurement of nanoparticle stability. The zeta potential of nanoparticle is the surface electric potential that arises due to tightly bound counter

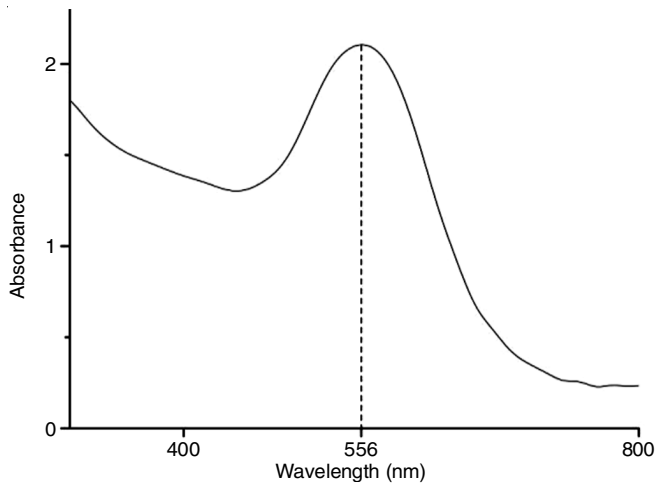


Fig. 1. UV-visible spectrum of HRP-AuNP conjugates

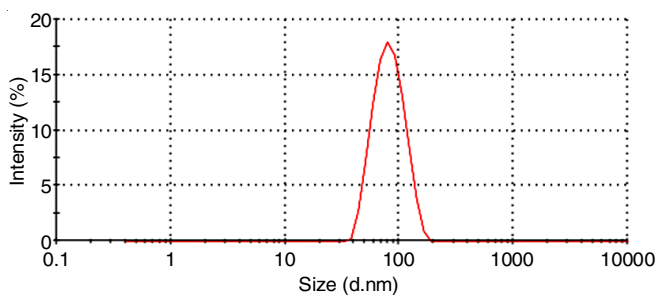


Fig. 2. Particle size based distribution of HRP-AuNP conjugates in tricine buffer

ion cloud that originates due to the conjugate layer and an outer diffused layer. Gold nanoparticle synthesized using HRP showed a potential of -18.4 ± 1.1 mV.

FTIR analysis: FTIR spectra of HRP and HRP-AuNP conjugate are shown in Fig. 3. In both spectra, a broad peak at 3409 cm^{-1} was observed which was assigned to the N-H stretching of amide group, present within the complex arrangement of HRP protein structure and implied the stabilization of particles by enzymes. Further, spectrum (b) exhibited an intense peak at 1660 cm^{-1} which is due to carbonyl group of amide linkage. Obtained results confirm the binding of HRP onto the surface of AuNP and acting as a stabilizing agent.

SEM and EDX analysis of HRP-AuNP conjugates: Size and morphology of HRP-AuNP conjugates was studied using SEM

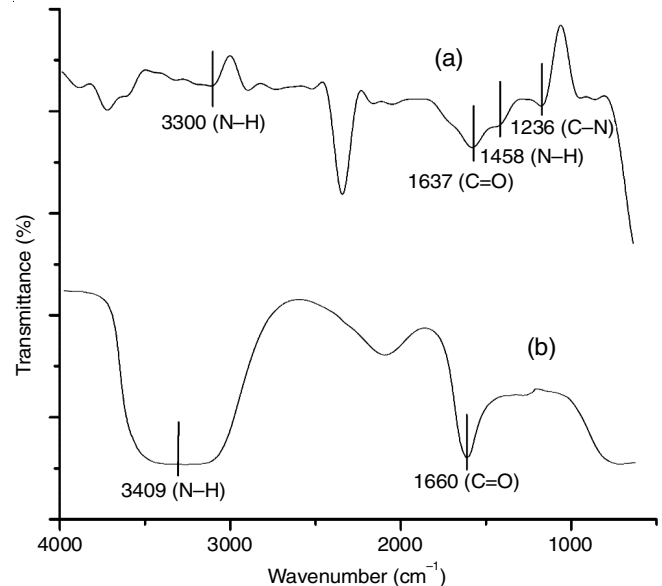


Fig. 3. FTIR spectra of (a) Free HRP and (b) HRP-AuNP conjugates

analysis. SEM images display that the particles were uniformly distributed thus indicating no agglomeration of the particles. Fig. 4a shows the HRP-AuNP conjugates as rounded particles having a particle size of 51.4 ± 5.5 nm. An average of four HRP-AuNP conjugates size was considered for calculating the standard deviation. EDX analysis of the particle system was done to determine the elemental composition of colloidal suspension. Fig. 4b clearly shows a strong peak at 2 keV which is a characteristic to AuNPs corresponding to its SPR absorption [50].

Enzyme kinetics studies

Steady state kinetics: Spectrophotometrically, kinetics of HRP in free form and its conjugated form as HRP-AuNP were determined [48] using Lineweaver-Burk equation. Activity of HRP was assayed by monitoring the oxidation of *o*-dianisidine, which upon reacting with H_2O_2 produces brown colored compound. Changes in optical density were recorded at 460 nm. Kinetic studies were done by varying the substrate concentration between 0.1 mM to 5mM, using initial rate method. The Michaelis-Menten constant value (K_m) was calculated in order to determine the affinity of enzyme for the substrate. The maximum enzyme activity (*i.e.* V_{max}) was also measured

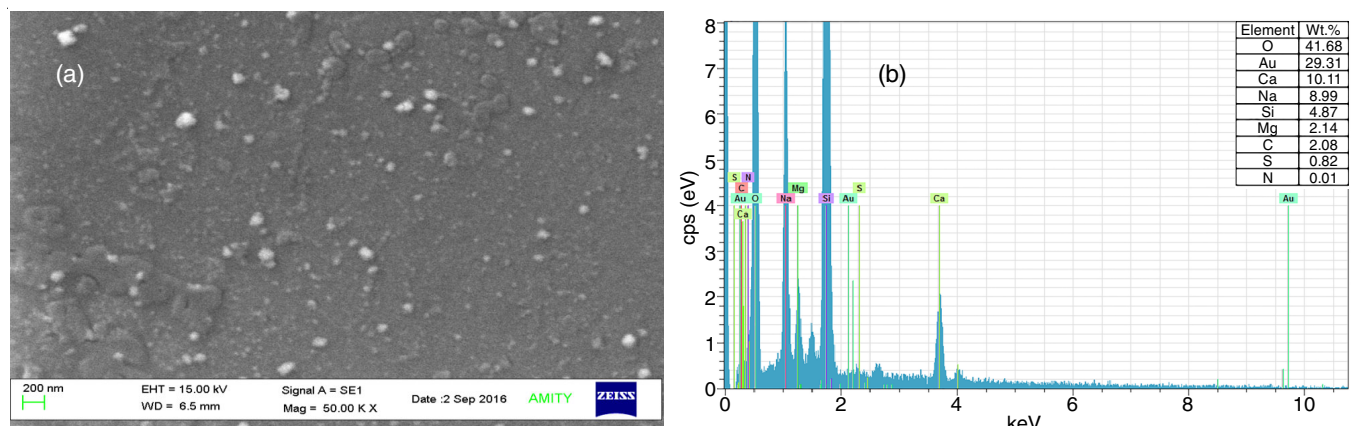


Fig. 4. (a) SEM images and (b) EDX spectrum of HRP-AuNP conjugates

TABLE-1
KINETICS PARAMETERS OF FREE HRP AND HRP-AuNP CONJUGATES

Sample	K_m (mM)	V_{max} (mM/min)	Specific activity ($\mu\text{mol}/\text{min}/\text{mg}$)	Immobilization (%)	Loading capacity	Loading efficiency (%)	Turnover number (s^{-1})
HRP	3.85	2.26	180.01	–	–	–	847.5
HRP-AuNP conjugates	1.81	5.70	454.01	208.82	0.81	97.0	2137.5

using the Lineweaver-Burk plot. A HRP-AuNP conjugate showed a lower K_m value (1.81 mM) as compared to free HRP (3.85 mM) indicating a better binding affinity of HRP towards substrate after conjugation to AuNP surface. The V_{max} of HRP-AuNP conjugate increased due to conjugation onto AuNP surface, which indicated a better availability of HRP active sites for binding to substrate (Table-1). Thus, overall better performance of HRP-AuNP conjugate suggested changes in primary structure of enzyme after conjugation with AuNPs.

Conclusion

In this study an easy and greener approach for biogenic synthesis of HRP-AuNP conjugates was adopted. It was shown that HRP enzyme can be used to synthesize gold nanoparticles at room temperature in tricine buffer. As evident from the various spectroscopic and imaging analysis, HRP was successfully conjugated to AuNPs and it was found to be mono-dispersed with a particle size of 51.4 ± 5.5 nm. It shows better enzyme activity than free HRP, which could be applicable as tag or labeling agent for various applications.

ACKNOWLEDGEMENTS

This work was supported by the Department of Biotechnology, New Delhi, India under a Bio-CARE Women Scientist Scheme Award to one of the authors (RS), [Grant No.BT/Bio-CARE/05/640/2011-12].

CONFLICT OF INTEREST

The authors declare that there is no conflict of interests regarding the publication of this article.

REFERENCES

- W.R. Glomm, *J. Dispers. Sci. Technol.*, **26**, 389 (2005); <https://doi.org/10.1081/DIS-200052457>
- R.A. Sperling, P. Rivera Gil, F. Zhang, M. Zanella and W.J. Parak, *Chem. Soc. Rev.*, **37**, 1896 (2008); <https://doi.org/10.1039/b712170a>
- P. Tiwari, K. Vig, V. Dennis and S. Singh, *Nanomaterials*, **1**, 31 (2011); <https://doi.org/10.3390/nano1010031>
- X. Huang, P.K. Jain, I.H. El-Sayed and M.A. El-Sayed, *Lasers Med. Sci.*, **23**, 217 (2008); <https://doi.org/10.1007/s10103-007-0470-x>
- K. Saha, S.S. Agasti, C. Kim, X. Li and V.M. Rotello, *Chem. Rev.*, **112**, 2739 (2012); <https://doi.org/10.1021/cr2001178>
- D.A. Giljohann, D.S. Seferos, W.L. Daniel, M.D. Massich, P.C. Patel and C.A. Mirkin, *Angew. Chem. Int. Ed.*, **49**, 3280 (2010); <https://doi.org/10.1002/anie.200904359>
- B. Sepúlveda, P.C. Angelomé, L.M. Lechuga and L.M. Liz-Marzán, *Nano Today*, **4**, 244 (2009); <https://doi.org/10.1016/j.nantod.2009.04.001>
- M. Fan, G.F. Andrade and A.G. Brolo, *Anal. Chim. Acta*, **693**, 7 (2011); <https://doi.org/10.1016/j.aca.2011.03.002>
- S. Maldonado, D. Knapp and N.S. Lewis, *J. Am. Chem. Soc.*, **130**, 3300 (2008); <https://doi.org/10.1021/ja800603v>
- M. Sengani, A.M. Grumezescu and V.D. Rajeswari, *OpenNano*, **2**, 37 (2017); <https://doi.org/10.1016/j.onano.2017.07.001>
- N. Elahi, M. Kamali and M.H. Baghersad, *Talanta*, **184**, 537 (2018); <https://doi.org/10.1016/j.talanta.2018.02.088>
- J. Turkevich, P.C. Stevenson and J. Hillier, *Discuss. Faraday Soc.*, **11**, 55 (1951); <https://doi.org/10.1039/d1f9511100055>
- G.K. Devi, P. Suruthi, R. Veerakumar, S. Vinoth, R. Subbaiya and S. Chozhavendhan, *Res. J. Pharm. Technol.*, **12**, 935 (2019); <https://doi.org/10.5958/0974-360X.2019.00158.6>
- G.A. Filip, B. Moldovan, I. Baldea, D. Olteanu, R. Suharoschi, N. Decea, C.M. Cismaru, E. Gal, M. Cenariu, S. Clichici and L. David, *J. Photochem. Photobiol. B*, **191**, 26 (2019); <https://doi.org/10.1016/j.jphotobiol.2018.12.006>
- M. Zou, J. Li, F. Zhang and Y. Jin, *Anal. Lett.*, **43**, 867 (2010); <https://doi.org/10.1080/00032710903486336>
- L. Wang, Y. Liu, W. Li, X. Jiang, Y. Ji, X. Wu, L. Xu, Y. Qiu, K. Zhao, T. Wei, Y. Li, Y. Zhao and C. Chen, *Nano Lett.*, **11**, 772 (2011); <https://doi.org/10.1021/nl103992v>
- S. Menon, R. S and V.K. S, *Resour.-Effic. Technol.*, **3**, 516 (2017); <https://doi.org/10.1016/j.reffit.2017.08.002>
- J.M. Slocik, R.R. Naik, M.O. Stone and D.W. Wright, *J. Mater. Chem.*, **15**, 749 (2005); <https://doi.org/10.1039/b413074j>
- Z. Vaseghi, A. Nematollahzadeh and O. Tavakoli, *Rev. Chem. Eng.*, **34**, 529 (2018); <https://doi.org/10.1515/revce-2017-0005>
- N. Noah, eds.: A.K. Shukla and S. Iravani, Green Synthesis: Characterization and Application of Silver and Gold Nanoparticles; In: Green Synthesis, Characterization and Applications of Nanoparticles, Elsevier, Chap. 6, pp. 111-135 (2019).
- S. Samanta, S. Agarwal, K.K. Nair, R.A. Harris and H. Swart, *Mater. Res. Express*, **6**, 082009 (2019); <https://doi.org/10.1088/2053-1591/ab296b>
- H.K. Daima, P. Selvakannan, Z. Homan, S.K. Bhargava and V. Bansal, Tyrosine Mediated Gold, Silver and Their Alloy Nanoparticles Synthesis: Antibacterial Activity Toward Gram Positive and Gram Negative Bacterial Strains; In: Nanoscience, Technology and Societal Implications (NSTSI), International Conference On IEEE (2011).
- Z. Wang, J. Zhang, J.M. Ekman, P.J. Kenis and Y. Lu, *Nano Lett.*, **10**, 1886 (2010); <https://doi.org/10.1021/nl100675p>
- H. Wei, Z. Wang, J. Zhang, S. House, Y.-G. Gao, L. Yang, H. Robinson, L.H. Tan, H. Xing, C. Hou, I.M. Robertson, J.-M. Zuo and Y. Lu, *Nat. Nanotechnol.*, **6**, 93 (2011); <https://doi.org/10.1038/nnano.2010.280>
- C.M. Niemeyer, *Angew. Chem. Int. Ed.*, **40**, 4128 (2001); [https://doi.org/10.1002/1521-3773\(20011119\)40:22<4128::AID-ANIE4128>3.0.CO;2-S](https://doi.org/10.1002/1521-3773(20011119)40:22<4128::AID-ANIE4128>3.0.CO;2-S)
- L. Rodríguez-Lorenzo, R. De La Rica, R.A. Álvarez-Puebla, L.M. Liz-Marzán and M.M. Stevens, *Nat. Mater.*, **11**, 604 (2012); <https://doi.org/10.1038/nmat3337>
- M. Sardar and J.A. Mazumder, eds.: N. Dasgupta, S. Ranjan and E. Lichtfouse, Biomolecules Assisted Synthesis of Metal Nanoparticles, in Environmental Nanotechnology, Springer International Publishing: Cham. vol. 2, p. 1-23 (2019).
- W. da Silva, M.E. Ghica, R.F. Ajayi, E.I. Iwuoha and C.M. Brett, *Food Chem.*, **282**, 18 (2019); <https://doi.org/10.1016/j.foodchem.2018.12.104>
- M. Peixoto de Almeida, P. Quaresma, S. Sousa, C. Couto, I. Gomes, L. Krippahl, R. Franco and E. Pereira, *Phys. Chem. Chem. Phys.*, **20**, 16761 (2018); <https://doi.org/10.1039/C8CP03116A>

30. I. Khan, R. Nagarjuna, J.R. Dutta and R. Ganesan, *Appl. Nanosci.*, **9**, 1101 (2018);
<https://doi.org/10.1007/s13204-018-0735-7>
31. M.A. Faramarzi and H. Forootanfar, *Colloids Surf. B Biointerfaces*, **87**, 23 (2011);
<https://doi.org/10.1016/j.colsurfb.2011.04.022>
32. L. Li and J. Weng, *Nanotechnology*, **21**, 305603 (2010);
<https://doi.org/10.1088/0957-4484/21/30/305603>
33. K. Govindaraju, V. Kiruthiga, R. Manikandan, T. Ashokkumar and G. Singaravelu, *Mater. Lett.*, **65**, 256 (2011);
<https://doi.org/10.1016/j.matlet.2010.09.078>
34. H. Kawasaki, K. Hamaguchi, I. Osaka and R. Arakawa, *Adv. Funct. Mater.*, **21**, 3508 (2011);
<https://doi.org/10.1002/adfm.201100886>
35. P. Ravindra, *Mater. Sci. Eng. B*, **163**, 93 (2009);
<https://doi.org/10.1016/j.mseb.2009.05.013>
36. S. Iravani, *Green Chem.*, **13**, 2638 (2011);
<https://doi.org/10.1039/c1gc15386b>
37. A. Rangnekar, T.K. Sarma, A.K. Singh, J. Deka, A. Ramesh and A. Chattopadhyay, *Langmuir*, **23**, 5700 (2007);
<https://doi.org/10.1021/la062749e>
38. B. Sharma, S. Mandani and T.K. Sarma, *J. Mater. Chem. B Mater. Biol. Med.*, **2**, 4072 (2014);
<https://doi.org/10.1039/C4TB00218K>
39. S.J. Lee, N. Scotti, N. Ravasio, I.S. Chung and H. Song, *Cryst. Growth Des.*, **13**, 4131 (2013);
<https://doi.org/10.1021/cg400949x>
40. P. Zhang, X.X. Yang, Y. Wang, N.W. Zhao, Z.H. Xiong and C.Z. Huang, *Nanoscale*, **6**, 2261 (2014);
<https://doi.org/10.1039/C3NR05269A>
41. A. Muthurasu and V. Ganesh, *RSC Adv.*, **6**, 7212 (2016);
<https://doi.org/10.1039/C5RA22477B>
42. F. Wen, Y. Dong, L. Feng, S. Wang, S. Zhang and X. Zhang, *Anal. Chem.*, **83**, 1193 (2011);
<https://doi.org/10.1021/ac1031447>
43. M. Zayats, R. Baron, I. Popov and I. Willner, *Nano Lett.*, **5**, 21 (2005);
<https://doi.org/10.1021/nl048547p>
44. X. Xu, M.S. Han and C.A. Mirkin, *Angew. Chem.*, **119**, 3538 (2007);
<https://doi.org/10.1002/ange.200605249>
45. X. Xie, W. Xu and X. Liu, *Acc. Chem. Res.*, **45**, 1511 (2012);
<https://doi.org/10.1021/ar300044j>
46. J. Oishi, Y. Asami, T. Mori, J.H. Kang, M. Tanabe, T. Niidome and Y. Katayama, *ChemBioChem*, **8**, 875 (2007);
<https://doi.org/10.1002/cbic.200700086>
47. D. Zhai, B. Liu, Y. Shi, L. Pan, Y. Wang, W. Li, R. Zhang and G. Yu, *ACS Nano*, **7**, 3540 (2013);
<https://doi.org/10.1021/nn400482d>
48. L.M. Shannon, E. Kay and J.Y. Lew, *J. Biol. Chem.*, **241**, 2166 (1966).
49. H. Jans, X. Liu, L. Austin, G. Maes and Q. Huo, *Anal. Chem.*, **81**, 9425 (2009);
<https://doi.org/10.1021/ac901822w>
50. W.-Y. Qiu, K. Wang, Y.-Y. Wang, Z.-C. Ding, L.-X. Wu, W.-D. Cai and J.-K. Yan, *Int. J. Biol. Macromol.*, **106**, 498 (2018);
<https://doi.org/10.1016/j.ijbiomac.2017.08.029>